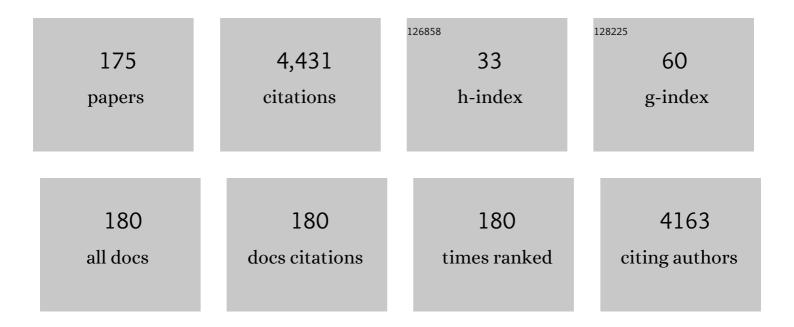
## **Michael Seibt**

List of Publications by Year in descending order

Source: https://exaly.com/author-pdf/7137307/publications.pdf Version: 2024-02-01



#	Article	IF	CITATIONS
1	Seebeck effect in magnetic tunnel junctions. Nature Materials, 2011, 10, 742-746.	13.3	260
2	Mechanisms of transition-metal gettering in silicon. Journal of Applied Physics, 2000, 88, 3795.	1.1	246
3	Electronic and chemical properties of the c-Si/Al2O3 interface. Journal of Applied Physics, 2011, 109, .	1.1	210
4	Photoluminescence of Carbon Nanodots: Dipole Emission Centers and Electron–Phonon Coupling. Nano Letters, 2014, 14, 5656-5661.	4.5	187
5	Room-temperature silicon light-emitting diodes based on dislocation luminescence. Applied Physics Letters, 2004, 84, 2106-2108.	1.5	166
6	Bandlike and localized states at extended defects in silicon. Physical Review B, 1995, 52, 13726-13729.	1.1	159
7	An approach to quantitative high-resolution transmission electron microscopy of crystalline materials. Ultramicroscopy, 1995, 58, 131-155.	0.8	139
8	Characterization of hazeâ€forming precipitates in silicon. Journal of Applied Physics, 1988, 63, 4444-4450.	1.1	119
9	Mapping projected potential, interfacial roughness, and composition in general crystalline solids by quantitative transmission electron microscopy. Physical Review Letters, 1993, 71, 4150-4153.	2.9	111
10	Disturbance of Tunneling Coherence by Oxygen Vacancy in Epitaxial <mml:math xmlns:mml="http://www.w3.org/1998/Math/MathML" display="inline"&gt;<mml:mi>Fe</mml:mi><mml:mo>/</mml:mo><mml:mi>MgO</mml:mi><mml:mo>/Tunnel Junctions. Physical Review Letters, 2008, 100, 246803.</mml:mo></mml:math 	> <mmi:mi></mmi:mi>	Fe?mml:mi>
11	Electrical and Recombination Properties of Copperâ€Silicide Precipitates in Silicon. Journal of the Electrochemical Society, 1998, 145, 3889-3898.	1.3	95
12	Electronic states at dislocations and metal silicide precipitates inÂcrystalline silicon and their role inÂsolar cell materials. Applied Physics A: Materials Science and Processing, 2009, 96, 235-253.	1.1	90
13	Tailored Synthetic Polyamines for Controlled Biomimetic Silica Formation. Journal of the American Chemical Society, 2010, 132, 1023-1031.	6.6	88
14	Microstructure-controlled magnetic properties of the bulk glass-forming alloy Nd60Fe30Al10. Applied Physics Letters, 2002, 80, 1749-1751.	1.5	83
15	Nucleation mechanism of the seed of tetrapod ZnO nanostructures. Journal of Applied Physics, 2005, 98, 034307.	1.1	82
16	Precipitation behaviour of nickel in silicon. Philosophical Magazine A: Physics of Condensed Matter, Structure, Defects and Mechanical Properties, 1989, 59, 337-352.	0.7	76
17	Structural and Electrical Properties of Metal Silicide Precipitates in Silicon. Physica Status Solidi A, 1999, 171, 301-310.	1.7	74
18	Recombination properties of structurally well defined NiSi2precipitates in silicon. Applied Physics Letters, 1991, 58, 911-913.	1.5	71

#	Article	IF	CITATIONS
19	Formation and Properties of Copper Silicide Precipitates in Silicon. Physica Status Solidi A, 1998, 166, 171-182.	1.7	67
20	Silicon light-emitting diodes based on dislocation-related luminescence. Physica Status Solidi (A) Applications and Materials Science, 2005, 202, 901-910.	0.8	60
21	Gettering in silicon photovoltaics: current state and future perspectives. Physica Status Solidi (A) Applications and Materials Science, 2006, 203, 696-713.	0.8	52
22	Regular Dislocation Networks in Silicon as a Tool for Nanostructure Devices used in Optics, Biology, and Electronics. Small, 2007, 3, 964-973.	5.2	50
23	Structural and electrical properties of metal impurities at dislocations in silicon. Physica Status Solidi (A) Applications and Materials Science, 2005, 202, 911-920.	0.8	47
24	Epitaxial growth of MgO and Feâ^•MgOâ^•Fe magnetic tunnel junctions on (100)-Si by molecular beam epitaxy. Applied Physics Letters, 2008, 93, .	1.5	45
25	Epitaxial growth of CuInS2 on sulphur terminated Si(001). Applied Physics Letters, 1998, 72, 2733-2735.	1.5	42
26	Impact of surface topography and laser pulse duration for laser ablation of solar cell front side passivating SiNx layers. Journal of Applied Physics, 2010, 108, 114514.	1,1	42
27	Preparation and properties of dc-sputtered IrO[sub 2] and Ir thin films for oxygen barrier applications in advanced memory technology. Journal of Vacuum Science & Technology an Official Journal of the American Vacuum Society B, Microelectronics Processing and Phenomena, 2001, 19, 1857.	1.6	41
28	Luminescence centres in silica nanowires. Nanotechnology, 2006, 17, 3215-3218.	1.3	41
29	P-type doping of GaAs nanowires. Applied Physics Letters, 2008, 92, 163107.	1.5	39
30	Phosphorous-diffusion gettering in the presence of a nonequilibrium concentrationof silicon interstitials: A quantitative model. Physical Review B, 1997, 55, 9577-9583.	1,1	38
31	Atomic structure and electronic states of nickel and copper silicides in silicon. Materials Science and Engineering B: Solid-State Materials for Advanced Technology, 2000, 72, 80-86.	1.7	36
32	Growth of β-FeSi2 films via noble-gas ion-beam mixing of Fe/Si bilayers. Journal of Applied Physics, 2001, 90, 4474-4484.	1.1	36
33	Simulation of Al and phosphorus diffusion gettering in Si. Materials Science and Engineering B: Solid-State Materials for Advanced Technology, 2000, 71, 175-181.	1.7	34
34	Influence of deposition conditions on Ir/IrO[sub 2] oxygen barrier effectiveness. Journal of Applied Physics, 2002, 91, 9591.	1.1	34
35	Structural and electronic properties of epitaxially grown CuInS 2 films. Thin Solid Films, 2000, 361-362, 504-508.	0.8	33
36	Cubic boron nitride thin film heteroepitaxy. Journal of Applied Physics, 2001, 90, 3248-3254.	1.1	33

#	Article	IF	CITATIONS
37	Self-organized nanoscale multilayer growth in hyperthermal ion deposition. Physical Review B, 2004, 70, .	1.1	32
38	Epitaxial growth and stress relaxation of vapor-deposited Fe–Pd magnetic shape memory films. New Journal of Physics, 2009, 11, 113054.	1.2	32
39	Quantitative strain mapping using high-resolution electron microscopy. Physica Status Solidi A, 1995, 150, 625-634.	1.7	31
40	Nanoscale Observation of a Grain Boundary Related Growth Mode in Thin Film Reactions. Physical Review Letters, 1998, 80, 774-777.	2.9	31
41	Microstructure and twinning in epitaxial NiMnGa films. Physical Review B, 2008, 78, .	1.1	30
42	Ion beam synthesis of diamond-like carbon thin films containing copper nanocrystals. Journal of Applied Physics, 2003, 93, 1203-1207.	1.1	29
43	PARAMETER SPACE FOR THERMAL SPIN-TRANSFER TORQUE. Spin, 2013, 03, 1350002.	0.6	29
44	Intrinsic luminescence and core structure of freshly introduced a-screw dislocations in n-GaN. Journal of Applied Physics, 2018, 123, .	1.1	26
45	Order and disorder in epitaxially grown CuInS2. Thin Solid Films, 2001, 387, 83-85.	0.8	25
46	Ion beam synthesis of amorphous carbon thin films containing metallic nanoclusters. Surface and Coatings Technology, 2002, 158-159, 114-119.	2.2	25
47	Electric breakdown in ultrathin MgO tunnel barrier junctions for spin-transfer torque switching. Applied Physics Letters, 2009, 95, .	1.5	25
48	Intra-atomic photoluminescence at 1.41 eV of substitutional Mn in GaMnN of high optical quality. Journal of Applied Physics, 2007, 101, 063504.	1.1	23
49	Sensitivity limits of strain mapping procedures using highâ€resolution electron microscopy. Journal of Microscopy, 1998, 190, 184-189.	0.8	22
50	Interaction of metal impurities with extended defects in crystalline silicon and its implications for gettering techniques used in photovoltaics. Materials Science and Engineering B: Solid-State Materials for Advanced Technology, 2009, 159-160, 264-268.	1.7	22
51	Oxygen tracer diffusion in IrO2 barrier films. Journal of Applied Physics, 2002, 91, 1707-1709.	1.1	21
52	Dendritic microstructure in the metallic glass matrix composite Zr56Ti14Nb5Cu7Ni6Be12. Scripta Materialia, 2005, 53, 93-97.	2.6	21
53	Self-organized pattern formation of biomolecules at silicon surfaces: Intended application of a dislocation network. Materials Science and Engineering C, 2006, 26, 902-910.	3.8	21
54	Selfâ€organized growth of InNâ€nanocolumns on pâ€5i(111) by MBE. Physica Status Solidi C: Current Topics in Solid State Physics, 2008, 5, 1706-1708.	0.8	21

#	Article	IF	CITATIONS
55	Electron microscopy analysis of crystalline silicon islands formed on screen-printed aluminum-doped p-type silicon surfaces. Journal of Applied Physics, 2008, 104, 043701.	1.1	21
56	Mechanisms and computer modelling of transition element gettering in silicon. Solar Energy Materials and Solar Cells, 2002, 72, 299-313.	3.0	20
57	Aluminum gettering of iron in silicon as a problem of the ternary phase diagram. Applied Physics Letters, 2009, 94, 061912.	1.5	20
58	Kinetics of ion-beam-induced interfacial amorphization in silicon. Journal of Applied Physics, 1997, 82, 5360-5373.	1.1	19
59	On the Role of Stacking Faults in Copper Precipitation in Silicon. Solid State Phenomena, 1991, 19-20, 45-50.	0.3	18
60	Elastic and inelastic conductance in Co-Fe-B/MgO/Co-Fe-B magnetic tunnel junctions. Physical Review B, 2010, 82, .	1.1	18
61	Cold nanoclusters on amorphous carbon synthesized by ion-beam deposition. Journal of Applied Physics, 2005, 98, 034304.	1.1	17
62	On the nature of defects produced by motion of dislocations in silicon. Physica Status Solidi (A) Applications and Materials Science, 2015, 212, 1695-1703.	0.8	16
63	Current–voltage characteristics of manganite–titanite perovskite junctions. Beilstein Journal of Nanotechnology, 2015, 6, 1467-1484.	1.5	16
64	Temperature dependent EBIC and deep level transient spectroscopy investigation of different types of misfit-dislocations at MOVPE grown GaAs/InGaAs/GaAs-single-quantum wells. Materials Science and Engineering B: Solid-State Materials for Advanced Technology, 1996, 42, 77-81.	1.7	15
65	Analysis of high resolution transmission electron microscope images of crystalline–amorphous interfaces. Ultramicroscopy, 2002, 90, 241-258.	0.8	15
66	Direct imaging of the structural change generated by dielectric breakdown in MgO based magnetic tunnel junctions. Applied Physics Letters, 2008, 93, 152508.	1.5	15
67	Electronic and structural properties of femtosecond laser sulfur hyperdoped silicon pn-junctions. Applied Physics Letters, 2013, 103, .	1.5	15
68	Spin-Transfer Torque Switching at Ultra Low Current Densities. Materials Transactions, 2015, 56, 1323-1326.	0.4	15
69	Atomic structure of the interface between silicon (111) and amorphous germanium. Physical Review B, 2004, 70, .	1.1	14
70	Influence of the Dislocation Travel Distance on the DLTS Spectra of Dislocations in Cz-Si. Solid State Phenomena, 2008, 131-133, 175-182.	0.3	14
71	Structure and Elemental Distribution of (Ga,Mn)N Nanowires. Nano Letters, 2011, 11, 398-401.	4.5	13
72	Influence of a ZnMnTe buffer layer on the growth of ZnTe on (001)GaAs by MOVPE. Journal of Crystal Growth, 2003, 249, 15-22.	0.7	12

#	Article	IF	CITATIONS
73	Ion energy thresholds and stability of cubic boron nitride. Diamond and Related Materials, 2003, 12, 1877-1882.	1.8	12
74	Structure, chemistry and electrical properties of extended defects in crystalline silicon for photovoltaics. Physica Status Solidi C: Current Topics in Solid State Physics, 2009, 6, 1847-1855.	0.8	12
75	Co-precipitation of copper and nickel in crystalline silicon. Materials Science and Engineering B: Solid-State Materials for Advanced Technology, 2009, 159-160, 365-368.	1.7	12
76	Synchrotron-based investigation of iron precipitation in multicrystalline silicon. Superlattices and Microstructures, 2009, 45, 168-176.	1.4	12
77	Structural and Electrical Properties of NiSi <sub>2</sub> Particles in Silicon. Solid State Phenomena, 1996, 47-48, 359-364.	0.3	11
78	Nanocrystallization of amorphous-Ta40Si14N46 diffusion barrier thin films. Applied Physics Letters, 2001, 78, 3618-3620.	1.5	11
79	Exploiting long-range atomic ordering for the investigation of strain relaxation in lattice-mismatched epitaxy. Applied Surface Science, 2002, 188, 61-68.	3.1	11
80	Co-rich magnetic amorphous films and their application in magnetoelectronics. Physical Review B, 2005, 72, .	1.1	11
81	Mn incorporation in GaN thin layers grown by molecular-beam epitaxy. Semiconductor Science and Technology, 2006, 21, 1348-1353.	1.0	11
82	High resolution imaging of extended defects in GaN using wave function reconstruction. Physica Status Solidi C: Current Topics in Solid State Physics, 2007, 4, 3010-3014.	0.8	11
83	Localization and preparation of recombination-active extended defects for transmission electron microscopy analysis. Review of Scientific Instruments, 2010, 81, 063705.	0.6	11
84	Light-induced point defect reactions of residual iron in crystalline silicon after aluminum gettering. Journal of Applied Physics, 2010, 108, 043519.	1.1	11
85	Tailoring the Absorption Properties of Black Silicon. Energy Procedia, 2012, 27, 480-484.	1.8	11
86	Contribution of Jahn-Teller and charge transfer excitations to the photovoltaic effect of manganite/titanite heterojunctions. New Journal of Physics, 2017, 19, 063046.	1.2	11
87	The Nature of the Electronic States of Cu <sub>3</sub> Si-Precipitates in Silicon. Solid State Phenomena, 1998, 63-64, 369-374.	0.3	10
88	Electrical Activity of Dislocations in Si Decorated by Ni. Solid State Phenomena, 2002, 82-84, 361-366.	0.3	10
89	Optimization of nanopores obtained by chemical etching on swift-ion irradiated lithium niobate. Nuclear Instruments & Methods in Physics Research B, 2009, 267, 1035-1038.	0.6	10
90	AUTOSAR-Compliant Development Workflows: From Architecture to Implementation - Tool Interoperability for Round-Trip Engineering and Verification and Validation. , 0, , .		10

#	Article	IF	CITATIONS
91	Formation of End-of-Range Defects in Silicon at Low Temperatures. Materials Research Society Symposia Proceedings, 1992, 262, 1103.	0.1	9
92	The temperature dependence of the ion beam induced interfacial amorphization in silicon. Applied Physics Letters, 1996, 68, 3425-3427.	1.5	9
93	Phosphorus Diffusion Gettering of Metallic Impurities in Silicon: Mechanisms beyond Segregation. Solid State Phenomena, 2004, 95-96, 527-538.	0.3	9
94	Self-assembled nano-scale multilayer formation using physical vapor deposition methods. Nuclear Instruments & Methods in Physics Research B, 2006, 242, 261-264.	0.6	9
95	Decomposition and metastable phase formation in the bulk metallic glass matrix composite Zr56Ti14Nb5Cu7Ni6Be12. Journal of Applied Physics, 2006, 99, 123519.	1.1	9
96	Interplay of Ni and Au Atoms with Dislocations and Vacancy Defects Generated by Moving Dislocations in Si. Solid State Phenomena, 0, 242, 147-154.	0.3	9
97	Generation of silicon nanocrystals by damage free continuous wave laser annealing of substrate-bound SiOx films. Journal of Applied Physics, 2015, 118, .	1.1	9
98	Phosphorus Diffusion Gettering of Platinum in Silicon: Formation of Near-Surface Precipitates. Physica Status Solidi (B): Basic Research, 2000, 222, 327-336.	0.7	8
99	Effect of Au contamination on the electrical characteristics of a "model―small-angle grain boundary in n-type direct silicon bonded wafer. Journal of Applied Physics, 2010, 108, 053719.	1.1	8
100	Temperature and bias-voltage dependence of atomic-layer-deposited HfO2-based magnetic tunnel junctions. Applied Physics Letters, 2014, 105, .	1.5	8
101	Epitaxial growth of gold on Si(001). Surface Science, 2014, 624, 15-20.	0.8	8
102	Phonon localization in ultrathin layered structures. Applied Physics A: Materials Science and Processing, 2015, 119, 11-18.	1.1	8
103	Recombination-related properties of a-screw dislocations in GaN: A combined CL, EBIC, TEM study. AIP Conference Proceedings, 2016, , .	0.3	8
104	Concerning vacancy defects generated by moving dislocations in Si. Materials Today: Proceedings, 2018, 5, 14757-14764.	0.9	8
105	Early stages of iron precipitation in silicon. Physica Status Solidi C: Current Topics in Solid State Physics, 2005, 2, 1802-1806.	0.8	7
106	Light-beam-induced current measurements on copper–nickel co-contaminated Cz-silicon bicrystals. Materials Science and Engineering B: Solid-State Materials for Advanced Technology, 2009, 159-160, 216-218.	1.7	7
107	Relaxation-Induced Gettering of Metal Impurities in Silicon: Microscopic Properties of Effective Gettering Sites. Materials Research Society Symposia Proceedings, 1992, 262, 957.	0.1	6
108	A metallic glass composite: Phase-field simulations and experimental analysis of microstructure evolution. Materials Science & Engineering A: Structural Materials: Properties, Microstructure and Processing, 2007, 452-453, 8-14.	2.6	6

#	Article	IF	CITATIONS
109	Combined XBIC/μâ€XRF/μâ€XAS/DLTS investigation of chemical character and electrical properties of Cu and Ni precipitates in silicon. Physica Status Solidi C: Current Topics in Solid State Physics, 2009, 6, 1868-1873.	0.8	6
110	Implantation of plasmonic nanoparticles in SiO2 by pulsed laser irradiation of gold films on SiO -coated fused silica and subsequent thermal annealing. Applied Surface Science, 2016, 374, 138-142.	3.1	6
111	Microscopic electronic and structural analysis of femtosecond laser sulfur hyperdoped silicon. Physica Status Solidi (A) Applications and Materials Science, 2017, 214, 1700264.	0.8	6
112	Room-Temperature Hot-Polaron Photovoltaics in the Charge-Ordered State of a Layered Perovskite Oxide Heterojunction. Physical Review Applied, 2020, 14, .	1.5	6
113	Epitaxial heterojunction devices. Solar Energy Materials and Solar Cells, 1997, 49, 337-342.	3.0	5
114	Structural and optical properties of $\hat{l}^2$ -FeSi2 layers grown by ion beam mixing. Surface and Coatings Technology, 2002, 158-159, 198-202.	2.2	5
115	Microstructural and Electrical Properties of NiSi <sub>2</sub> Precipitates at Dislocations in Silicon. Solid State Phenomena, 2004, 95-96, 447-452.	0.3	5
116	Electrical properties of gold at dislocations in silicon. Physica Status Solidi C: Current Topics in Solid State Physics, 2005, 2, 1847-1851.	0.8	5
117	Nanofabrication of spin-transfer torque devices by a polymethylmethacrylate mask one step process: Giant magnetoresistance versus single layer devices. Journal of Applied Physics, 2007, 101, 104302.	1.1	5
118	Impact of NiSi <sub>2</sub> Precipitates Electronic Structure on the Minority Carrier Lifetime in n-and p-Type Silicon. Solid State Phenomena, 2007, 131-133, 155-160.	0.3	5
119	Long-range order on the atomic scale induced at CoFeB/MgO interfaces. Journal of Applied Physics, 2009, 105, 073701.	1.1	5
120	Orbital-order phase transition in <mml:math xmlns:mml="http://www.w3.org/1998/Math/MathML"&gt; <mml:mrow> <mml:msub> <mml:mi>Pr</mml:mi> <mml:mr probed by photovoltaics. Physical Review B, 2021, 103, .</mml:mr </mml:msub></mml:mrow></mml:math 	.0 <b>₩</b> ⊅ < mm	l:man>1
121	Depth Dependence of Dislocation Loop Dissolution Kinetics in Ion Implanted Silicon. Solid State Phenomena, 1997, 57-58, 377-382.	0.3	4
122	Nonconservative Ostwald ripening of dislocation loops in silicon. Applied Physics Letters, 1998, 73, 2956-2958.	1.5	4
123	Phase separation and magnetic properties of Nd60Fe30Al10 thin films. Applied Physics Letters, 2004, 85, 2565-2567.	1.5	4
124	Nanostructure of chemically phase separated La–Ce–Mn–O thin films. Applied Physics Letters, 2007, 91, 132508.	1.5	4
125	Electrical properties of gold in dislocated silicon. Physica Status Solidi (A) Applications and Materials Science, 2007, 204, 2185-2189.	0.8	4
126	Deposition and properties of high-carbon iron films. Applied Surface Science, 2007, 254, 955-960.	3.1	4

#	Article	IF	CITATIONS
127	Comparison of Efficiency and Kinetics of Phosphorus-Diffusion and Aluminum Gettering of Metal Impurities in Silicon: a Simulation study. Solid State Phenomena, 0, 156-158, 229-234.	0.3	4
128	Self-organized formation of layered carbon–copper nanocomposite films by ion deposition. Nuclear Instruments & Methods in Physics Research B, 2009, 267, 1356-1359.	0.6	4
129	Tunnel magnetoresistance in alumina, magnesia and composite tunnel barrier magnetic tunnel junctions. Journal of Magnetism and Magnetic Materials, 2011, 323, 1525-1528.	1.0	4
130	Electron microscopy of an aluminum layer grown on the vicinal surface of a gallium arsenide substrate. Semiconductors, 2015, 49, 337-344.	0.2	4
131	Quantitative assessment of molecular dynamics-grown amorphous silicon and germanium films on silicon (111). Surface Science, 2016, 651, 100-104.	0.8	4
132	Graphene quantum dots with visible light absorption of the carbon core: insights from single-particle spectroscopy and first principles based theory. 2D Materials, 2016, 3, 041008.	2.0	4
133	High-resolution Scanning Transmission EBIC Analysis of Misfit Dislocations at Perovskite pn-Heterojunctions. Journal of Physics: Conference Series, 2019, 1190, 012009.	0.3	4
134	Behaviour of the Size Distribution Function of End-of-Range Dislocation Loops during Silicon Oxidation. Solid State Phenomena, 1996, 47-48, 205-210.	0.3	3
135	High-Temperature Properties of Transition Elements in Silicon. , 0, , 597-660.		3
136	Interaction of Interstitially Dissolved Cobalt and Oxygen-Related Centres in Silicon. Solid State Phenomena, 2004, 95-96, 553-558.	0.3	3
137	Substitutional-to-interstitial ratio of manganese in nanostructured GaN by electron channeling enhanced microanalysis. Journal of Applied Physics, 2008, 103, 073520.	1.1	3
138	Localisation and identification of recombination-active extended defects in crystalline silicon by means of focused ion-beam preparation and transmission electron microscopy. Physica Status Solidi C: Current Topics in Solid State Physics, 2009, 6, 1862-1867.	0.8	3
139	Platinum and gold diffusion monitor vacancy profiles induced into silicon wafers by aluminum alloying. Physica Status Solidi (A) Applications and Materials Science, 2013, 210, 771-776.	0.8	3
140	The influence of the atomic structure of basal planes on interplanar distance in pyrolytic carbon materials. Technical Physics Letters, 2016, 42, 1137-1140.	0.2	3
141	Low energy scanning transmission electron beam induced current for nanoscale characterization of p–n junctions. Physica Status Solidi - Rapid Research Letters, 2017, 11, 1600358.	1.2	3
142	Microstructural analysis of the modifications in substrate-bound silicon-rich silicon oxide induced by continuous wave laser irradiation. Journal of Alloys and Compounds, 2017, 707, 227-232.	2.8	3
143	Extended core structure and luminescence of a-screw dislocations in GaN. Journal of Physics: Conference Series, 2019, 1190, 012006.	0.3	3
144	Environmental transmission electron microscopy study of hydrogen charging effect on a Cu-Zr metallic glass. Materials Research Letters, 2020, 8, 439-445.	4.1	3

#	Article	IF	CITATIONS
145	The effect of the translational symmetry of crystalline silicon on the structure of amorphous germanium in the interfacial region. Crystallography Reports, 2004, 49, 225-232.	0.1	2
146	High-Resolution Electron Microscopy of Interfaces between Solids with Varying Degree of Atomic Ordering. Journal of Materials Science, 2004, 12, 311-319.	1.2	2
147	Electrical Properties of Clustered and Precipitated Iron in Silicon. Solid State Phenomena, 2005, 108-109, 109-114.	0.3	2
148	Transmission Electron Microscopy Investigations of Metal-Impurity-Related Defects in Crystalline Silicon. Solid State Phenomena, 2011, 178-179, 275-284.	0.3	2
149	Interaction of Iron with Extended Defects in Multicrystalline Silicon Studied by Local Gettering. Energy Procedia, 2013, 38, 582-588.	1.8	2
150	Mesoscopic properties of interfacial ordering in amorphous germanium on Si(111) determined by quantitative digital image series matching. Ultramicroscopy, 2013, 126, 1-9.	0.8	2
151	Turbostratic pyrocarbon structure study by means of exit wave reconstruction from high-resolution transmission electron microscopy. Physica Status Solidi C: Current Topics in Solid State Physics, 2015, 12, 1179-1182.	0.8	2
152	Preparation Techniques for Crossâ€Section Transmission Electron Microscopy Lamellas Suitable for Investigating In Situ Silicon–Aluminum Alloying at Grain Boundaries in Multicrystalline Silicon. Physica Status Solidi (A) Applications and Materials Science, 2019, 216, 1900308.	0.8	2
153	Correlation of structure and intrinsic luminescence of freshly introduced dislocations in GaN revealed by SEM and TEM. AIP Conference Proceedings, 2019, , .	0.3	2
154	Phase Transitions in a Perovskite Thin Film Studied by Environmental In Situ Heating Nanoâ€Beam Electron Diffraction. Small Methods, 2021, 5, e2100464.	4.6	2
155	Investigation of oxygen diffusion barrier properties of reactively sputtered iro2 thin films. Integrated Ferroelectrics, 2001, 37, 29-38.	0.3	1
156	Pattern Recognition in High-Resolution Electron Microscopy of Complex Materials. Microscopy and Microanalysis, 2006, 12, 476-482.	0.2	1
157	Influence of the Mn compositional distribution on the magnetic order in diluted GaMnN layers. Physica Status Solidi C: Current Topics in Solid State Physics, 2008, 5, 1832-1835.	0.8	1
158	Transmission electron microscopy analysis of extended defects in multicrystalline silicon using in-situ EBIC/FIB sample preparation. Physica Status Solidi C: Current Topics in Solid State Physics, 2013, 10, 32-35.	0.8	1
159	Characterization of Electrical Contacts on Silicon (100) after Ablation and Sulfur Doping by Femtosecond Laser Pulses. Solid State Phenomena, 2013, 205-206, 358-363.	0.3	1
160	Structural studies of Al thin layer on misoriented GaAs(100) substrate by transmission electron microscopy. Physica Status Solidi C: Current Topics in Solid State Physics, 2015, 12, 1148-1151.	0.8	1
161	Electron microscopy study of turbostratic pyrolytic carbon atomic structure using the exit wave reconstruction technique. Bulletin of the Russian Academy of Sciences: Physics, 2015, 79, 1353-1359.	0.1	1
162	Formation of porous silicon oxide from substrate-bound silicon rich silicon oxide layers by continuous-wave laser irradiation. Journal of Applied Physics, 2018, 123, .	1.1	1

#	Article	IF	CITATIONS
163	A posteriori synchronization of scanning transmission electron microscopy signals with kilopixel per second acquisition rates. Ultramicroscopy, 2019, 200, 62-66.	0.8	1
164	Recombination and Charge Collection at Nickel Silicide Precipitates in Silicon Studied by Electron Beamâ€Induced Current. Physica Status Solidi (B): Basic Research, 2021, 258, 2100142.	0.7	1
165	Site-specific plan-view TEM lamella preparation of pristine surfaces with a large field of view. Ultramicroscopy, 2021, 228, 113320.	0.8	1
166	Nucleation of nickel disilicide precipitates in floatâ€≢one silicon: the role of vacancies. Physica Status Solidi (A) Applications and Materials Science, 0, , .	0.8	1
167	Measurement of the ratio of substitutional to interstitial dopant-incorporation in nanostructures. Microscopy and Microanalysis, 2007, 13, 428-429.	0.2	Ο
168	Electron microscopy analysis of silicon islands and line structures formed on screen-printed Al-doped p <sup>+</sup> -surfaces. Conference Record of the IEEE Photovoltaic Specialists Conference, 2008, , .	0.0	0
169	Charge pattern formation at silicon surfaces for defined biomolecule adsorption. AIP Conference Proceedings, 2008, , .	0.3	0
170	Spatially Resolved Defect Analysis in Cz-Silicon after Copper-Nickel Co-Precipitation by Virtue of Light-Beam-Induced Current Measurements. Solid State Phenomena, 0, 156-158, 431-436.	0.3	0
171	Study of the structure and composition of the strained epitaxial layer in the InAlAs/GaAs(100) heterostructure by transmission electron microscopy. Semiconductors, 2016, 50, 1753-1758.	0.2	Ο
172	Phase Transitions in a Perovskite Thin Film Studied by Environmental In Situ Heating Nanoâ€Beam Electron Diffraction (Small Methods 9/2021). Small Methods, 2021, 5, 2170042.	4.6	0
173	Structural Investigation of Amorphous/Crystalline Interfaces by Iterative Digital Image Series Matching. , 2008, , 155-156.		0
174	Transmission Electron Microscopy Investigation of Self-Organized InN Nano-columns. , 2008, , 93-94.		0
175	Dendritic Microstructure, Decomposition, and Metastable Phase Formation in the Bulk Metallic Glass Matrix Composite Zr56Ti14Nb5Cu7Ni6Be12. , 0, , 407-420.		Ο